

Volume Profiles for the Reversible Binding of Dioxygen to Cobalt(II) Complexes. Evidence for a Substitution-Controlled Process

Menglin Zhang,[†] Rudi van Eldik,^{*,‡} James H. Espenson,^{*,†} and Andreja Bakac^{*,†}

Ames Laboratory and the Department of Chemistry, Iowa State University, Ames, Iowa 50011, and Institute for Inorganic Chemistry, University of Witten/Herdecke, 58488 Witten, Germany

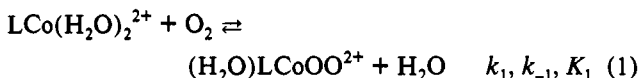
Received July 30, 1993[⊙]

The rate constants for the binding and release of dioxygen from two cobalt(II) macrocycles have been determined in aqueous solution as a function of pressure at 25.0 °C. The products of these reactions are L^1CoOO^{2+} and L^2CoOO^{2+} , where L^1 = cyclam and L^2 = hexamethylcyclam. The pressure dependence of the equilibrium constant for the L^2 system was also evaluated, giving $\Delta V^\circ = -22.0 \pm 0.4$ mL mol⁻¹. The binding rate constants have $\Delta V^\ddagger = +0.4 \pm 0.5$ mL mol⁻¹ (L^1) and -4.7 ± 0.3 mL mol⁻¹ (L^2). The reverse reaction for L^2CoOO^{2+} has $\Delta V^\ddagger = +17.9 \pm 0.5$ mL mol⁻¹. The volume profile is presented for the L^2 system, from which an interchange mechanism for substitution at Co(II) is proposed. Electron transfer is not significantly advanced at the transition state. The reverse reaction, release of dioxygen from the cobalt(III)–superoxo complex, has a large positive value of ΔV^\ddagger , consistent with the electron transfer preceding the partial dissociation of O_2 .

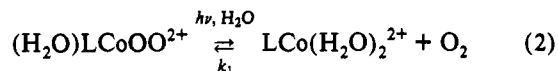
Introduction

The reversible binding of dioxygen to metal complexes continues to be an active subject.¹ This is particularly so for cobalt–oxygen interactions, since such adducts are active in arene oxidations,² in alkane autoxidations,³ and as models for dioxygenase.⁴

Volume profiles are now a well-recognized method that aids in the resolution of the reaction mechanism, particularly as regards the extent of bond-making and bond-breaking in the transition state.^{5,6} This work reports the determination of the volume profile for one such interaction and a partial determination for the second. These cobalt–oxygen reactions are ones that we have considered previously.⁷ The equilibrium and kinetic situation for L^2 is described by eq 1,



For $L^1 = [14]aneN_4$, the formation of the μ -peroxo complex complicates the picture, such that $(H_2O)L^1CoO_2^{2+}$ and $((H_2O)L^1CoOOCOL^1(H_2O))^{4+}$ are the major species present in oxygen-containing solutions. However, as shown earlier,⁷ only $(H_2O)L^1CoO_2^{2+}$ can be photodissociated in a laser flash, and the subsequent reequilibration is equivalent to that for the L^2 system. Thus for both L^1 and L^2 we have the following:



The results of this study allow us to comment on the nature of the transition state for the binding of dioxygen to these Co(II) complexes and the extent to which bond formation is accompanied

by electron transfer to produce the $Co^{III}-O_2^-$ species. Furthermore, a comparison can be made with volume profiles recently reported for the binding of alkyl radicals to $Co^{II}(nta)(H_2O)_2^-$ and $Cr(H_2O)_6^{2+}$, processes that are controlled by solvent exchange at the metal center.^{8,9}

Experimental Section

The ligands and the salt $[L^2Co](CF_3SO_3)_2$ and the solution species $L^1Co(H_2O)_2^{2+}$ were prepared as previously described.^{7,10} Both of the complexes have the cobalt atom located at the center of the N_4 plane of the macrocycle. There are presumably two water molecules in the axial positions in place of the perchlorate anions that are found in these positions in the solid perchlorate salts.¹¹ Oxygen concentrations were established by the careful dilution of a saturated (1.27 mM) solution in water. This was done without agitation, the solutions being made up in a cuvette or vial with very little gas space. This was then transferred to the high-pressure "pillbox" cuvette for the kinetic measurements at elevated pressures.

The kinetic experiments were carried out by laser flash photolysis, and equilibrium measurements by spectrophotometry, since the $(H_2O)-LCoOO^{2+}$ adducts show intense absorption bands near 330 nm. Samplings of the previously-reported kinetics and equilibrium experiments at atmospheric pressure were repeated inside the special high-pressure cell^{12,13} and found to agree entirely with those values. The system was then pressurized at various pressures of 50–2000 atm, and similar measurements were made. The total dissolved oxygen concentration remained constant at elevated pressure since no gas bubbles were present in the sample cell prior to pressurization. Furthermore, the "pillbox" technique¹³ employed does not require any absorbance correction for changes in concentration during compression of the solution, since the optical pathlength decreases in the same manner. Fresh solutions were prepared immediately prior to each determination, since the oxygenated solutions began to degrade after 30–60 min.

Results

Equilibrium Measurements. The reaction between $L^2Co(H_2O)_2^{2+}$ and O_2 is reversible. Even at the highest concentration

[†] Iowa State University.

[‡] University of Witten/Herdecke.

[⊙] Abstract published in *Advance ACS Abstracts*, December 1, 1993.

- (1) Sheldon, R. A.; Kochi, J. K. *Metal-Catalyzed Oxidations of Organic Compounds*; Academic Press: New York, 1981; Chapters 1, 2, and 4.
- (2) (a) Sheldon, R. A.; Kochi, J. K. *Adv. Catal.* **1970**, *25*, 272. (b) Brill, W. F. *Ind. Eng. Chem.* **1960**, *52*, 837. (c) Hay, A. S.; Eustance, J. W.; Blanchard, H. S. *J. Org. Chem.* **1960**, *25*, 616.
- (3) Onopchenko, A.; Schulz, J. G. D. *J. Org. Chem.* **1978**, *38*, 909; **1978**, *38*, 3729.
- (4) Nishinaga, A.; Nishizawa, K.; Tomita, H.; Matsuura, T. *J. Am. Chem. Soc.* **1977**, *99*, 1287.
- (5) van Eldik, R.; Asano, T.; le Noble, W. J. *Chem. Rev.* **1989**, *89*, 549–688.
- (6) van Eldik, R.; Merbach, A. E. *Comments Inorg. Chem.* **1992**, *12*, 341.
- (7) Bakac, A.; Espenson, J. H. *J. Am. Chem. Soc.* **1990**, *112*, 2273.

- (8) van Eldik, R.; Cohen, H.; Meyerstein, D. *Angew. Chem., Int. Ed. Engl.* **1991**, *30*, 1158.

- (9) van Eldik, R.; Gaede, W.; Cohen, H.; Meyerstein, D. *Inorg. Chem.* **1992**, *31*, 3695.

- (10) Bakac, A.; Espenson, J. H. *Inorg. Chem.* **1989**, *28*, 3901; **1989**, *28*, 4319.

- (11) (a) Endicott, J. F.; Lilie, J.; Kusaj, J. M.; Ramaswamy, B. S.; Schmonsees, W. G.; Simic, M. G.; Glick, M. D.; Rillema, D. P. *J. Am. Chem. Soc.* **1977**, *99*, 429. (b) Bakac, A.; Espenson, J. H. *Inorg. Chem.* **1990**, *29*, 2062.

- (12) Spitzer, M.; Gärtig, F.; van Eldik, R. *Rev. Sci. Instrum.* **1988**, *59*, 2092.

- (13) le Noble, W. J.; Schlott, R. *Rev. Sci. Instrum.* **1976**, *47*, 770.

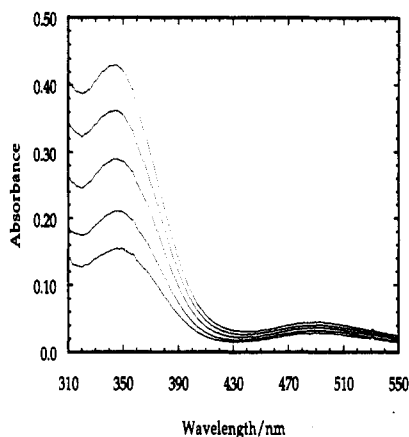


Figure 1. Sample of the spectral intensification upon application of high pressure to the equilibrium system containing $L^2Co(H_2O)_2^{2+}$, O_2 , and $(H_2O)L^2Co(O_2)^{2+}$. The concentrations are $[Co]_T = 2.00 \times 10^{-4}$ M and $[O_2]_e = 0.75$ mM. The pressures, reading upward, are 1, 500, 1000, 1500, and 2000 atm.

Table 1. Pressure-Dependent Equilibrium Data^a for the Reaction $L^2Co(H_2O)_2^{2+} + O_2(aq) \rightleftharpoons L^2Co(O_2)(H_2O) + H_2O$

<i>p</i> /atm	<i>K</i> ^b		
	at $[O_2] = 0.25$ mM	at $[O_2] = 0.75$ mM	at $[O_2] = 1.25$ mM
1	378, 378	370, 473	370, 370
500	554, 578	568, 732	594, 556
1000	907, 907	945, 1189	965, 926
1500	1416, 1346	1439, 1952	1621, 1481
2000	2134, 2041	2131, 3067	2361, 2325

^a At 25.0 °C, with $[O_2]$ in the units mol L⁻¹; $L^2 = Me_6[14]aneN_4$. ^b *K* in units L mol⁻¹ from duplicate determinations under each set of conditions.

of O_2 , 1.25 mM, only about 30% of the total cobalt exists as the superoxo complex at atmospheric pressure.⁷ When this system is placed under 2000 atm pressure, the strong absorbance of the superoxo complex ($\lambda_{max} = 343$ nm, $\epsilon = 2.4 \times 10^3$ L mol⁻¹ cm⁻¹)⁷ increases to a value that is 3.6 times greater than that at $p = 1$ atm. These spectral changes are shown in Figure 1. The $L^2Co(H_2O)_2^{2+}$ complex has a negligible absorbance ($\epsilon < 10^2$ L mol⁻¹ cm⁻¹) throughout the spectral region shown.

From the absorbances at various pressures and at different concentrations of $L^2Co(H_2O)_2^{2+}$ and O_2 , equilibrium constants were calculated. They are collected in Table 1. The value at $p = 1$ atm is $K_1 = 3.78 \times 10^2$ L mol⁻¹, which compares well with 3.70×10^2 L mol⁻¹ reported previously.⁷

The equilibrium constant rises fairly sharply with pressure, consistent with the spectral intensifications recorded. The variation of $\ln K_1$ with pressure is shown in Figure 2. The relation is linear as expected from the thermodynamic relation in eq 3.

$$\ln K = \ln K^\circ - (\Delta V^\circ/RT)p \quad (3)$$

Least-squares fitting gives a value of the standard molar volume change, $\Delta V^\circ = -22.0 \pm 0.4$ mL mol⁻¹, for the six experiments reported in Table 1. When ΔV° is calculated for each experiment separately, the average value is -22.4 ± 0.4 mL mol⁻¹.

Kinetics of L^2Co^{2+} . The flash photolysis technique was used to follow the rate of this reaction. Photolysis of an equilibrated mixture causes partial dissociation of oxygen, followed by the re-equilibration⁷ which obeys the kinetics of eq 4.⁷

$$k_e = k_1\{[O_2]_e + [L^2Co^{2+}]_e\} + k_{-1} \quad (4)$$

It is not meaningful to analyze the pressure dependence of k_e itself, since it is the composite shown. This means that at each pressure different sets of concentrations must be used to define k_1 and k_{-1} . The results are presented in Table 2, where each entry represents the average of 4–8 determinations. Figure 3

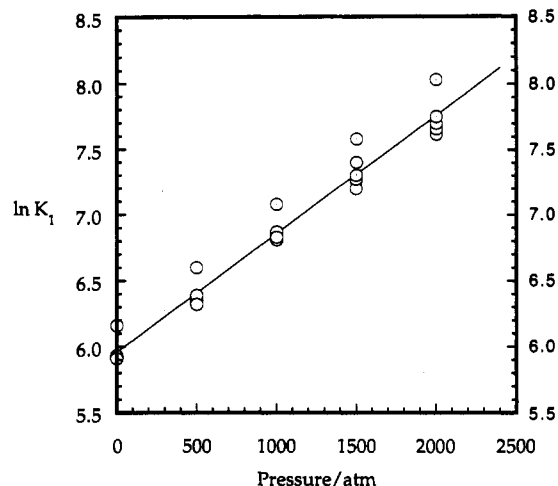


Figure 2. Analysis of the pressure dependence of the equilibrium constant K_1 for $L^2Co(H_2O)_2^{2+}$ and $(H_2O)L^2Co(O_2)^{2+}$, shown as a plot of $\ln K_1$ versus pressure. This gives $\Delta V^\circ = -22.0$ mL mol⁻¹.

Table 2. Data for the Kinetics of Equilibration^a of the Reaction $L^2Co(H_2O)_2^{2+} + O_2(aq) \rightleftharpoons (H_2O)L^2Co(O_2)^{2+} + H_2O$

$[L^2Co]_T/\mu M$	$[O_2]_T/\mu M$	<i>p</i> /atm				
		1	500	1000	1500	2000
180	250	1.79	1.27	0.937	0.731	0.600
150	550	1.92	1.46	1.07	0.89	0.75
200	750	2.03	1.58	1.17	1.00	0.88
200	1000	2.14	1.67	1.30	1.14	1.04
200	1250	2.22	1.75	1.43	1.28	1.18

^a In H_2O at 25.0 °C. Entries are values of $k_e/10^4$ s⁻¹.

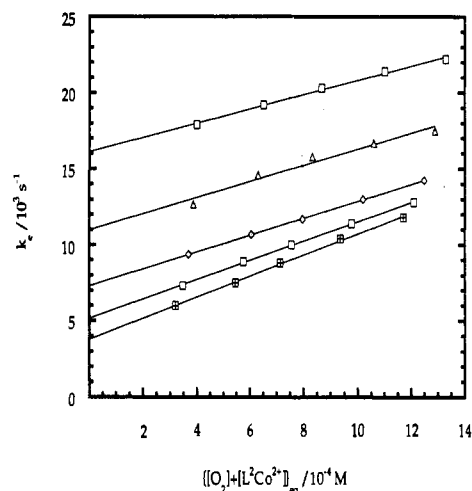


Figure 3. Equilibration rate constant for the $L^2Co(H_2O)_2^{2+}/(H_2O)L^2Co(O_2)^{2+}$ system shown as a linear function of the sum of the equilibrium concentrations at a given pressure. The slope is k_1 , and the intercept k_{-1} , as given by eq 4. The pressures, reading downward, are 1, 500, 1000, 1500, and 2000 atm.

shows the plot of k_e versus $\{[O_2]_e + [L^2Co^{2+}]_e\}$ at each pressure. To construct this plot the equilibrium concentrations were calculated from the value of K_1 at the given pressure and the total concentrations that are specified in Table 2.

Least-squares fits to eq 4 give these values:

<i>p</i> /atm	1	500	1000	1500	2000
$k_1/10^6$ L mol ⁻¹ s ⁻¹	4.68	5.28	5.55	6.35	6.93
$k_{-1}/10^4$ s ⁻¹	1.61	1.10	0.732	0.518	0.379

The pressure dependence of each rate constant follows the expected form, eq 5. The plots of $\ln k_i$ versus p are shown in Figure 4. Least-squares analysis gives these volumes of activa-

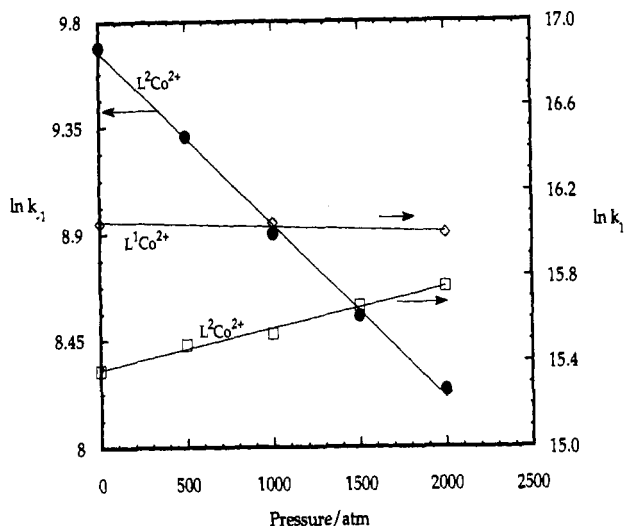


Figure 4. Plots of $\ln k$ versus p for k_1 and k_{-1} for the reaction $L^2Co(H_2O)_2^{2+} + O_2 \rightleftharpoons L^2Co(O_2)(H_2O)_2^{2+} + H_2O$ and for k_1 in the analogous reaction of the L^1 system.

tion: $\Delta V_1^\ddagger = -4.7 \pm 0.3 \text{ mL mol}^{-1}$ and $\Delta V_{-1}^\ddagger = +17.9 \pm 0.5 \text{ mL mol}^{-1}$. The combination of these yields $\Delta V^\circ = \Delta V_1^\ddagger - \Delta V_{-1}^\ddagger = -22.6 \pm 0.8 \text{ mL mol}^{-1}$, which agrees excellently with the value determined directly from the equilibrium measurements.

$$\ln k_i = \ln k_i^\circ - (\Delta V_i^\ddagger / RT)p \quad (5)$$

Kinetics of L^1Co^{2+} . This reaction is, for all intents and purposes, unidirectional, with the equilibrium in eq 1 lying far to the right.⁷ In that case, only the forward direction of the reaction is revealed through the kinetic analysis. In view of that the general expression in eq 4 is simplified by the elimination of the k_{-1} term. At each pressure, as found earlier at atmospheric pressure, a plot of the experimental rate constant against $[O_2]_{av}$ is a straight line that passes through the origin.

The kinetic data show an extremely modest pressure effect. Indeed, the plot of $\ln k_1$ versus pressure, which is also given in Figure 4, is seen to be nearly horizontal. Least-squares analysis gives $\Delta V^\ddagger = +0.4 \pm 0.7 \text{ mL mol}^{-1}$.

Discussion

The kinetic data recorded for the binding of dioxygen to $L^2Co(H_2O)_2^{2+}$ following the flash (Table 2) show a significant decrease in k_2 with increasing pressure. In many of the kinetic experiments the concentrations of the reactants were comparable, such that eq 4 defines the observed rate constant for the approach to equilibrium. The graphic presentation of the data in Figures 3 and 4 indicates that the intercept (k_{-1}) decreases significantly with increasing pressure, whereas the effect on the slope (k_1) is small. These trends result in the significantly positive and small negative volumes of activation, respectively, and allow us to construct a volume profile for the reversible binding of dioxygen to $L^2Co(H_2O)_2^{2+}$ as shown in Figure 5.

By way of comparison, the binding of dioxygen to $L^1Co(H_2O)_2^{2+}$ exhibits no pressure dependence and the volume of activation is practically zero. In both systems the binding of dioxygen involves displacement of a coordinated solvent (water) molecule and an electron-transfer process during which the metal center is oxidized to cobalt(III) and dioxygen reduced to superoxide ion. What is the nature of the transition state for this process?

The volume profile in Figure 5 indicates that the transition state for the binding of dioxygen has a partial molar volume close to that of the reactants. The small values of ΔV^\ddagger found for these reactions indicate that ligand substitution on the cobalt(II) center controls the binding process. In the case of $L^1Co(H_2O)_2^{2+}$, a

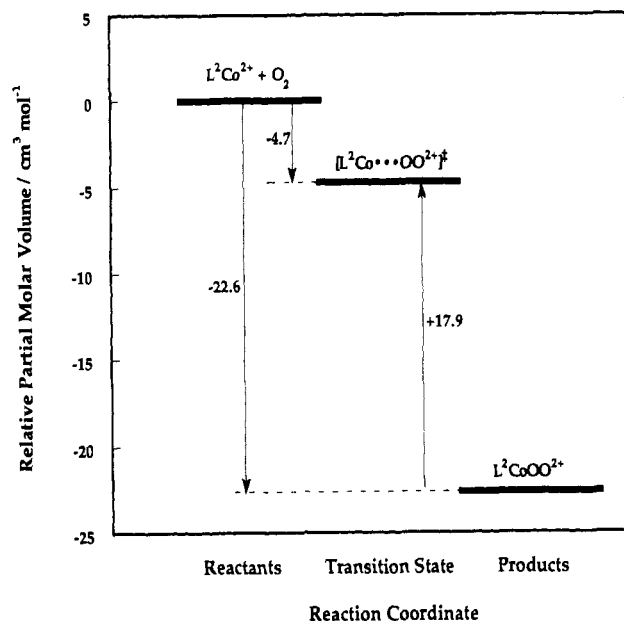


Figure 5. Volume profile, showing the changes in partial molar volume along the reaction coordinate for the reaction $L^2Co(H_2O)_2^{2+} + O_2 \rightleftharpoons (H_2O)L^2Co(O_2)^{2+} + H_2O$.

volume collapse associated with the bond formation with dioxygen is canceled by a volume increase associated with the release of a coordinated solvent molecule. This process can therefore be described as a pure interchange of ligands in the transition state; *i.e.*, neither bond formation nor bond breaking dominates in determining the overall ΔV^\ddagger value. In the case of $L^2Co(H_2O)_2^{2+}$, the volume collapse is not totally canceled by the volume increase. There are various possible reasons for this difference between the two systems. The $Me_6\text{cyclam}$ (L^2) complex, being much bulkier than the cyclam (L^1) complex, will sweep out a much larger volume due to its rotational movement. The partial release of a coordinated solvent molecule will cause a smaller volume increase than in the case of the less bulky L^1 system.

The available reduction potentials¹⁴ favor the oxidation of $L^1Co(H_2O)_2^{2+}$ more than the oxidation of $L^2Co(H_2O)_2^{2+}$. Thus if the electron transfer would contribute to the transition state, a more negative ΔV^\ddagger value would be expected for the binding of dioxygen to $L^1Co(H_2O)_2^{2+}$ than to $L^2Co(H_2O)_2^{2+}$. This is not the case, however, and we conclude that electron transfer does not contribute significantly to the transition state. During the bond formation between $Co(II)$ and O_2 , the coordinated solvent molecule is fully released from the coordination sphere. This is followed by an intramolecular electron transfer process to form $Co^{III}-O_2^-$. It is the latter process that accounts for the large volume collapse on the way to the products. Thus the binding of dioxygen is a ligand-substitution-controlled process, followed by a much faster intramolecular electron-transfer reaction.

During the release of O_2 , the large positive ΔV^\ddagger value results from the reduction of $Co(III)$ to $Co(II)$ and oxidation of O_2^- to O_2 and the partial dissociation of O_2 . The overall reaction volume of $-22.6 \text{ mL mol}^{-1}$ is close to that found for the binding of the $\cdot\text{CH}_3$ radical to $Co^{II}(\text{nta})(H_2O)_2^-$ ($-16.4 \text{ mL mol}^{-1}$),⁸ once the difference in the partial molar volumes of O_2 and $\cdot\text{CH}_3$ is taken into consideration. The volume profile in the latter case consists of a volume increase of $+2.2 \text{ mL mol}^{-1}$ between the reactants and the transition state followed by a volume collapse of $-18.6 \text{ mL mol}^{-1}$ between the transition state and the products. The volume increase in the process of bond formation was interpreted in terms of a dissociative interchange (I_d) ligand substitution reaction dominated by the $Co-OH_2$ bond cleavage. This is followed by

(14) (a) Liteplo, M. P.; Endicott, J. F. *Inorg. Chem.* **1971**, *10*, 1420. (b) Heckman, R. E.; Espenson, J. H. *Inorg. Chem.* **1979**, *18*, 38.

the large volume collapse caused by the binding of CH₃ and the oxidation of Co^{II}-CH₃[•] to Co^{III}-CH₃⁻.⁸ In another series of studies,⁹ it was found that the reaction of 10 different aliphatic free radicals with Cr(H₂O)₆²⁺ to produce (H₂O)₅Cr-R²⁺ takes place with $\Delta V^{\ddagger} = +4.3 \pm 1.0$ mL mol⁻¹. Again this was interpreted in terms of a solvent-exchange-controlled process, facilitated by the Jahn-Teller distortion on Cr(II), followed by the Cr-R bond formation. For the actual binding of [•]C(CH₃)₂OH following the transition state, a volume collapse of -15.1 mL mol⁻¹ was reported,¹⁵ which is probably due to the contraction of the metal center during electron transfer, Cr^{II}-R[•] → Cr^{III}-R⁻. It follows from a comparison of these volume profiles with that found in this study that the binding of dioxygen and aliphatic radicals to Co(II) and Cr(II) takes place by similar mechanisms, in which ligand substitution (*i.e.*, the displacement of coordinated water) controls the nature of the transition state.

In systems in which there is a vacant coordination site, such as in model heme complexes, the binding of dioxygen is

accompanied by a significantly negative ΔV^{\ddagger} value, which is -11.3 mL mol⁻¹ for the monochelated protoheme system,¹⁶ due to the volume collapse associated with bond formation. Similarly, the binding of dioxygen to an Ir(I) complex in an oxidative addition process is characterized by a very negative ΔV^{\ddagger} value of -31 ± 2 mL mol⁻¹, partly due to the bond formation and partly due to the oxidation of Ir(I) to Ir(III).¹⁷ Thus, the saturated coordination sphere of the Co(II) complexes studied here requires the partial dissociation of a coordinated solvent molecule in terms of an interchange process prior to bond formation.

Acknowledgment. This work was supported by the U.S. Department of Energy, Office of Basic Energy Sciences, Chemical Sciences Division, under Contract W-7405-Eng-82. R.v.E. kindly acknowledges financial support from the Volkswagen Foundation that enabled him to participate in this study.

(15) Sisley, M. J.; Rindermann, W.; van Eldik, R.; Swaddle, T. W. *J. Am. Chem. Soc.* **1984**, *106*, 7432.

(16) Taube, D. J.; Projahn, H. D.; van Eldik, R.; Magde, D.; Traylor, T. G. *J. Am. Chem. Soc.* **1990**, *112*, 6880.

(17) de Waal, D. J. A.; Gerber, T. I. A.; Louw, W. J.; van Eldik, R. *Inorg. Chem.* **1982**, *21*, 2002.